

FMSG: Cyber: Self-Learning Robotic Epitaxy for Superconducting Quantum Circuitry

1 Introduction

1.1 Major Challenges in Manufacturing Superconducting Quantum Materials and Circuits

Superconducting materials, where electricity is carried with zero resistance and a macroscopic quantum state is maintained, are foundational to the manufacturing of quantum circuitry and quantum computers. However, the manufacturing of superconducting materials and quantum circuitry has met major challenges. **First**, the fabrication of even seemingly simple superconducting materials is associated with an enormous parameter space. For instance, to optimize a binary superconductor (*e.g.*, TiN, NbN, FeSe) one needs to consider at least the fluxes of two elements, substrate temperature, pre-

and post-growth annealing temperatures and durations, let alone the various parameters associated with subsequent lithographic processing. Fully exploring this high-dimensional parameter space will require the fabrication of $> 10^7$ samples, which cannot be completed within a reasonable time frame. **Second**, superconductivity is a delicate quantum phenomenon [1, 2, 3]. Subtle differences in the initial condition of substrates can lead to drastically different electronic properties of superconducting thin films, making the traditional Bayesian optimization based on a fixed input-output mapping difficult to implement. **Third**, the historical development of superconductors relied on serendipitous discoveries. The discovery of high-temperature copper-oxide superconductors was considered heretical as Bednorz and Müller started with insulators instead of conductors [4]. Progress can be stagnant for manufacturing new superconducting quantum materials and quantum circuits, if we always rely on the “old wisdom” which confines the available parameter space.

1.2 Mission Statement

In this Future Manufacturing Seed Grant (FMSG) project, we will develop preliminary prototypes of self-learning robotic epitaxy for manufacturing high-temperature thin film superconductors, and robotic mini-epitaxy for manufacturing superconducting quantum circuits. We will specifically focus on monolayer FeSe thin-film superconductors, as their fabrication embodies the major challenges for superconductor manufacturing: large parameter space, extreme sensitivity to initial conditions, and opportunities for optimization out of the traditional parameter space. The project involves two stages of manufacturing. In wafer-scale robotic epitaxy, we will feed the real-time electron diffraction data into a structured reinforcement learning (RL) algorithm, and guide the entire synthesis process with real-time optimization. This is distinct from the traditional Bayesian optimization, where fixed growth parameters are identified for all material manufacturing. Our RL algorithm will treat each substrate according to its initial condition, making real-time adjustments and mimicking the operation of an experienced human operator. In the sub-micrometer-scale robotic mini-epitaxy, we will leverage a unique technique for quantum circuit manufacturing, miniaturized molecular beam epitaxy (mini-MBE) developed in the Yang laboratory, where molecular beams are confined by sub-micrometer nozzles and the substrate is controlled by a piezosscanner with nanometer precision. By

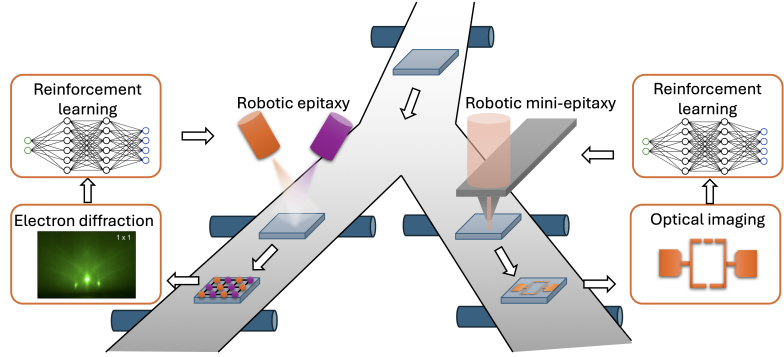


Figure 1: **Schemes of robotic epitaxy to manufacture quantum materials and robotic mini-epitaxy to manufacture quantum devices.** In robotic epitaxy, real-time electron diffraction data is fed into a reinforcement learning algorithm to guide the robotic system’s trajectory in the parameter space. In robotic mini-epitaxy, real-time optical imaging data is fed into another reinforcement learning algorithm to maintain the optimal conditions for printing the desired superconducting quantum circuits.

programming the piezosscanner to move in specific patterns, quantum circuits will be printed without resorting to any lithographic processing, tremendously saving the manufacturing cost, energy consumption, and environmental consequences for making each quantum bit (qubit). A unique challenge is how to ensure optimal deposition in different local regions. We will feed real-time optical images to an RL algorithm, which adjusts the printing speed and the nozzle-substrate distance to ensure high-quality superconducting device printing. It is important to note that these optical images serve as real-time indirect indicators of device quality, thus functioning as the reward mechanism for training the RL agent. To enrich this process, we plan to integrate the thin-film deposition recipe learned in the wafer-scale robotic epitaxy. Eventually, the new knowledge we obtain in this FMSG project will pave the foundation for further development of high-fidelity local characterization in robotic mini-epitaxy, such as micro-focused electron diffraction, which will enable a completely new manufacturing modality for printing quantum circuits using a broad class of superconductor materials (e.g., Aluminum, Tantalum, etc.). Such extended activities will naturally fall within the scope of a Future Manufacturing full grant.

1.3 How Artificial Intelligence Helps

The integration of AI with cybermanufacturing signifies a transformative advancement for future manufacturing, fueled by vast amounts of data available, substantial computational resources, and notable advancements in the algorithms, mathematics, and statistics that underpin AI technologies. Our objective is to harness these developments to revolutionize cybermanufacturing processes, making them more adaptive, efficient, and capable of handling complex challenges.

Active Learning (AL) Helps Effectively Sample the Parameter Space AL plays a critical role in optimizing the cyber manufacturing process. Traditional heuristic-driven approaches often fall short where domain knowledge is insufficient to inform the next design, and classical AL approaches struggle with the scale and complexity of possible manufacturing variables, largely due to their reliance on low-dimensional data and limited scalability. Advanced AL techniques help mitigate such limitations, by combining representation learning, uncertainty quantification, and approximation algorithms for combinatorial optimization to effectively navigate the extensive parameter spaces involved.

Reinforcement Learning (RL) Helps Adapt to Different Initial Conditions RL continuously explores the parameter space, making decisions based on the results of past actions to efficiently navigate through “uncharted territories” of the manufacturing process. Leveraging deep RL tools, we can transform the original massive experimental design space into a structured policy space induced by the RL value functions. This structure allows more efficient exploration and adaptive MBE control in real-time, optimizing operations in response to both internal variables and external influences.

1.4 Enabling Future Manufacturing

Catalyzing New Manufacturing Capabilities The standard protocol for manufacturing superconducting qubits has been the sequence of synthesizing superconducting films such as Aluminum using electron-beam evaporation, followed by a tedious nanoscale lithographic process involving harsh chemical treatments, ultraviolet irradiation, and electron beam irradiation. Our proposed activities will realize RL-driven automatic film fabrication and RL-driven lithography-free quantum circuit printing. Such manufacturing capabilities do not exist yet, and will be enabled by the fundamental research on robotic epitaxy and how it is integrated with structured RL. The robotic mini-epitaxy will realize qubit printing without the need of nanofabrication, which will transform the manufacturing of superconducting qubits and superconducting quantum computers.

Significant Impacts of the Proposed Research in Cyber and Eco Manufacturing Despite the rapid development of artificial intelligence (AI) and robotic material processing, AI-informed material manufacturing has been focused on soft and bio-materials [5, 6, 7, 8]. The application of AI on hard quantum materials and quantum devices has been limited. The fundamental difference is that the properties of soft and bio-materials are determined by statistical averages over large thermal, chemical, and structural fluctuations, and that the

properties of quantum materials result from the delicate quantum coherent states which are sensitive to small differences in the initial conditions and complex trajectories in the fabrication parameter space. By developing structured RL algorithms providing real-time instructions to a robotic epitaxy system, our research will enable the first systematic application of RL-informed manufacturing on superconducting materials and devices, and have a transformative impact on *cyber manufacturing*. By developing RL algorithms to guide robotic mini-epitaxy to print superconducting qubits, our research will yield the fundamental knowledge base to manufacture qubits and quantum computers without traditional nanofabrication. This will significantly reduce the time, energy, chemical consumption, and environmental impact of every qubit. As a rough estimate, using the current nanofabrication technology each chip made of tens of superconducting qubits takes ~ 200 fabrication hours in a high-grade clean room, which incurs not only 10^3 's dollars but also 10^4 's kW.h of energy. Our robotic mini-epitaxy will thus have a significant impact on *eco manufacturing* of quantum devices.

Interdisciplinary Team Our team is co-led by a thin-film materials scientist (**Yang**) and a computer scientist (**Chen**). The successful implementation of robotic epitaxy and mini-epitaxy requires a seamless integration of their respective expertise. This is demonstrated by their preliminary success in implementing robotic epitaxy of silver beamsplitters as shown in Section 2.4.

Global Context of the Proposed Research The U.S. is no longer the dominant player in the world in advanced thin-film deposition. The industrial labs that sponsored the great materials revolutions of the last century, such as Bell Labs and IBM Research, are no longer supporting materials discovery and crystal growth. Recent major discoveries in thin-film materials, such as the Quantum Spin Hall Effect [9] and the Quantum Anomalous Hall Effect [10], were made in Germany and in China, respectively. The Japanese materials science community has pioneered in machine-learning (ML)-informed quantum materials synthesis on SrRuO₃ [11, 12, 13] and TiN [14], as well as the classification of surface reconstructions on GaAs [15]. There is a strong urgency to accelerate the fundamental research in ML-driven quantum materials synthesis in the U.S. to reestablish the American competitiveness in advanced precision fabrication.

Impact on the Economy, Labor Force, and Society at Large AI and quantum technologies are two important areas for economy and job growth. McKinsey Global Institute estimates that AI can deliver a global economical output of \$13 trillion/year by 2030 [16]. The Chicago Quantum Exchange, of which PI **Yang** is a member, is leading the *Bloch Tech Hub*, a coalition of industry, academic, government, and nonprofit stakeholders to develop quantum technologies. The Bloch Tech Hub has been named an official U.S. Regional Innovation and Technology Hub, with the State of Illinois committing \$500 million investment. This technology hub is expected to generate \$60 billion economic growth, create 30,000 quantum jobs, train 50,000 workers, and support 200 quantum companies by 2035 [17]. Our proposed research will potentially transform how superconducting qubits and quantum computers are manufactured, with a direct impact in this emerging quantum technology center and the quantum economy at large.

2 Research Description

Our *grand vision* is to construct an automated deposition system at sub-micrometer scale and realize the equivalent of an AI-driven 3D printer for superconducting quantum devices. Toward this long-term goal, we propose research activities for two stages of integration between AI and robotic epitaxy. For the first stage, we will develop structured RL algorithms to optimize the superconducting properties of wafer-scale monolayer FeSe thin films based on real-time characterization using reflection high-energy electron diffraction (RHEED). *Objectives 1 and 2* will enable the collection of RHEED data and facilitate the development of structured RL, respectively. For the second stage, we will leverage the originally developed mini-MBE setup in the Yang laboratory, and develop RL algorithms to achieve the optimal uniformity of printed superconducting circuitry such as Josephson junctions and transmons. Notably, the data and models we generate in *Objectives 1 and 2* will form the basis of coarse-grained learning on which *Objective 3* is constructed. For the seed grant period, we will utilize optical microscopy data for real-time feedback and control in robotic mini-epitaxy. We will specifically focus on the growth of monolayer FeSe superconductors on SrTiO₃ sub-

strates [18, 19, 20]. We emphasize that the new knowledge we generate on real-time control of thin-film epitaxy and nanoscale printing will be generalizable to other thin-film quantum materials.

Objective 1: Build the Multi-Stage Epitaxy Database for Structured RL The first milestone is to feed massive real-time characterization data to structured RL models. In MBE, RHEED provides convenient real-time characterizations, yet the interpretation of RHEED data often relies on experienced MBE operators and requires multiple years of training. For *Objective 1*, we will use a prototypical system – monolayer FeSe superconductor grown on SrTiO₃ substrate [18, 20, 21, 22, 23, 24, 25, 26, 27]. This material was chosen due to its structural simplicity and strong dependence on specific growth conditions. We will efficiently explore the parameter space using *Active Learning*. The data will be key to the supervised learning in *Objective 2*.

Objective 2: Design Structured Deep RL Models to Guide Self-Learning Robotic Epitaxy We aim to leverage the structure of our experimental setups to refine the efficiency of robotic epitaxy using a novel structured deep RL framework. This approach not only facilitates more intuitive navigation through the complex parameter space but also enables the generation of new, nested environments that reflect the real-world progression of epitaxial growth. To ensure a thorough exploration of this structured parameter space, we will leverage off-the-shelf offline RL tools [28, 29, 30, 31, 32, 33, 34] to pre-train a collection of deep RL policies from the data collected from *Objective 1*, and then develop an active policy search algorithm to guide the global exploration of the structured design space. This balanced methodology of local exploration (via deep RL) and global exploration (through active policy search) aims to streamline the search for optimal growth conditions and enhance the control and understanding of material synthesis processes.

Objective 3: Develop Preliminary RL Models for Real-Time Control in Robotic Mini-Epitaxy. We will leverage the mini-MBE setup that was originally developed in the Yang laboratory, and integrate it with a customized RL model adapted from the bi-level RL literature [35, 36, 37, 38, 39] for real-time control of deposition conditions, scanning speed, and nozzle-substrate distance. Given the limited time and resources of the FMSG, we will use optical imaging with $\sim 1 \mu\text{m}$ resolutions, providing low-fidelity characterization data for the RL model. Josephson junctions, which are fundamental building blocks of qubits and quantum computers, will be printed by robotic mini-epitaxy. This objective will yield fundamental scientific and engineering insights into how to realize a 3D printer of superconducting qubits. The full potential of the RL model will be exploited in the Future Manufacturing full proposal, where micro-focused electron sources will be developed to facilitate micro-RHEED as the high-fidelity characterization technique.

2.1 Objective 1: Build the Multi-Stage Epitaxy Database for Structured RL

2.1.1 Introduction of the FeSe Growth Process on SrTiO₃ Substrate

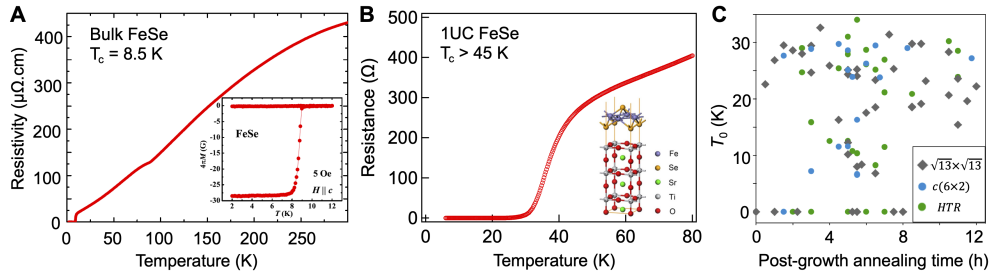


Figure 2: Interfacial enhancement of superconductivity in 1 UC FeSe/STO. (A) Resistivity measurement on bulk FeSe characterizing the transition temperature (T_c) close to 8.5 K. The inset illustrates the diamagnetism concomitant with the superconducting transition. (B) Resistance measurement on 1UC FeSe/STO showing a $T_c > 45 \text{ K}$. (C) Scattered zero-resistance temperature T_0 as a function of the post-growth annealing time. Different symbols represent different STO reconstruction patterns. The T_0 results are scattered with no obvious pattern.

One-unit-cell thick FeSe grown on SrTiO₃(100), or 1 UC FeSe/STO, is a unique material platform that exhibits fascinating superconducting properties. Bulk FeSe is an unconventional superconductor with a moderate transition temperature (T_c) of 8.5 K [40, 41], whereas 1 UC FeSe/STO exhibits a $T_c > 45 \text{ K}$

according to electrical transport [20], and a $T_c > 70$ K by Scanning Tunneling Spectroscopy (STS) [18] and Angle-Resolved Photoemission Spectroscopy (ARPES) [21, 22, 23, 24, 25]. Here we emphasize that this material serves as an exemplary system which showcases how material qualities can sensitively depend on the specific growth conditions. For instance, Fig. 2 shows that the zero-resistance T_c can scatter in a wide range between 0 and 50 K without obvious correlations with substrate reconstructions or post-growth annealing time. We emphasize that this fact does not suggest that there is no way to control the FeSe growth, but instead demonstrates that the characterization results are complex functions of growth parameters. For instance, optimization of the post-growth annealing time may depend on the quality of the as-grown FeSe film; optimization of the growth parameters can rely on the substrate state after the pre-growth annealing.

We emphasize that the multi-stage growth protocol and the extreme sensitivity to the prior-stage status make the epitaxial growth of 1 UC FeSe/STO, as well as many delicate superconducting materials, not suitable for traditional ML modeling such as Bayesian optimization [11, 12]. The optimal growth process needs to be defined according to the initial condition and all subsequent system states. This is also a primary reason for the difficulty in mass-producing high-quality 1 UC FeSe/STO films for quantum applications - the optimal growth process needs the operator to make real-time decisions at each stage of the growth, and such decisions have been made by experienced human operators. To truly transform the superconducting film growth into a *manufacturing* production line, we need to develop the fundamental AI tools to accommodate different initial and intermediate conditions and generate real-time instructions to enable robotic epitaxy. The growth process can be summarized in a tree *structure* as shown in Fig. 3.

Pre-growth substrate annealing. The FeSe growth starts with a delicate treatment of the STO substrate. STO has a pseudo-cubic structure and a strong tendency to form a wide variety of different surface reconstructions [42, 43, 44]. A surface reconstruction such as $c(4 \times 2)$ is characterized by a periodic distortion on the surface layer which has a period four times the lattice constant along one axis and twice along the orthogonal axis. STO can be heat-treated using different conditions to achieve $c(2 \times 1)$, $c(4 \times 2)$, $c(4 \times 4)$, $c(6 \times 2)$, ($\sqrt{13} \times \sqrt{13}$ -R33.7°) reconstructions [42, 43, 44]. These reconstructions can be characterized directly by RHEED, which forms the database to train ML models later. Importantly, the FeSe quality sensitively depends on the specific surface reconstruction, which in turn depends on the pre-growth annealing condition defined by the annealing temperature (T_{pre}) and duration (D_{pre}).

Epitaxial growth. FeSe grows in the so-called absorption-control mode, for which a Se overpressure is required to grow high-quality FeSe. There is no consensus in the literature on the exact Fe:Se ratio, which ranges from 1:4 [20, 21, 27] to 1:10 [18, 22, 23, 24, 45]. Moreover, the Fe flux determines the growth speed (seconds/layer). There is also no consensus in the literature on the growth speed, ranging from 30 seconds/layer [20, 21, 27] to > 10 minutes/layer [18, 22, 23, 24, 45]. The control parameters for this stage are the Fe and Se fluxes (F_{Fe} , F_{Se}), as well as the substrate temperature (T_S).

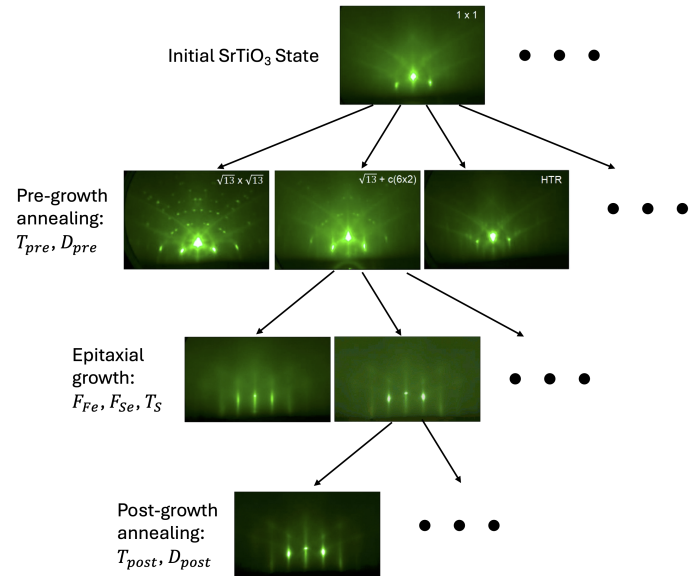


Figure 3: The structure of the growth recipe for 1 UC FeSe/STO. Excluding the initial condition, the recipe is composed of 3 stages: pre-growth annealing (annealing temperature T_{pre} , annealing duration D_{pre}), epitaxial growth (Fe flux F_{Fe} , Se flux F_{Se} , substrate temperature T_S), and post-growth annealing (annealing temperature T_{post} , annealing duration D_{post}). The RHEED results at each stage depend on not only the growth parameters at the same stage, but also the ending state from the previous stage.

Post-growth film annealing. 1 UC FeSe/STO as grown is often insulating. To achieve high T_c , the last key parameters for the growth recipe are the temperature (T_{post}) and duration (D_{post}) for post-growth film annealing. During this annealing, a few important physical processes occur: excess Se will evaporate from the FeSe surface; the crystallinity of FeSe will be further improved; most importantly, the interfacial interaction between the FeSe film and the STO substrate is substantially enhanced.

In this FMSG project, we will develop a structured RL framework (with model development described in *Objective 2*) to accommodate the structure of the epitaxial growth process. In *Objective 1*, we will build the comprehensive structured RHEED database at different stages of the growth process, as shown in Fig. 3, exploring a wide range for all seven growth parameters. Notably, this new AI development will allow us to efficiently explore the hierarchical structure of the design space, and tailor the RL algorithm to generate instructions for different initial and intermediate states, which resolves one fundamental challenge in manufacturing superconducting materials. On the other hand, the data structure will also enable us to efficiently explore the parameter space outside the traditional “wisdom” by properly balancing exploration and exploitation at different levels of the hierarchy. This new capability allows for serendipitous discoveries outside the parameter range defined by previous experiments, which resolves another general challenge in applying AI to quantum materials synthesis. Finally, this development will also provide the training data to form the coarse-grained *environmental conditions* for the real-time control of robotic mini-epitaxy in *Objective 3*.

Justification for using RHEED data for robotic epitaxy of optimal superconducting films: RHEED provides the direct and *in situ* characterization of material qualities. Different surface reconstructions on STO substrates and different states of 1 UC FeSe films are both directly reflected in RHEED images (Fig. 3). Fig. 4 depicts the evolution of RHEED images for a continuous sequence of post-growth annealing at 450 °C, and compares it with the evolution of the superconducting onset T_c , or T_{onset} . When the signal-to-background ratio increases, and sharp dots start to develop on the ±1st-order diffraction peaks, T_{onset} also increases and reaches the maximum. This experiment justifies using RHEED data as real-time feedback for robotic epitaxy of optimal FeSe films.

2.1.2 Active Learning for RHEED Data Generation

Metric for Success Use active learning to generate 500 ~ 1,000 RHEED images on STO and FeSe during the 2-year FMSG grant period for offline training of structured RL.

The growth process of 1 UC FeSe/STO is defined by 7 parameters (Fig. 3). For a passive exhaustive search in the 7-dimensional parameter space with at least 10 sampling points along each dimension, we will need to fabricate 10^7 samples. Instead, we will utilize *Active Learning* in the RHEED data generation, in which we use Gaussian Process Regression (GPR) to model the mapping between adjacent stages in the multi-stage data structure. For each training iteration, we sample new growth parameters where the GPR model has the largest standard deviation for prediction. We emphasize that this active learning algorithm is used to generate the needed pre-collected data for offline RL training. This algorithm allows us to search in the *input data space*. It is fundamentally different from the *Active Policy Search* for online RL training

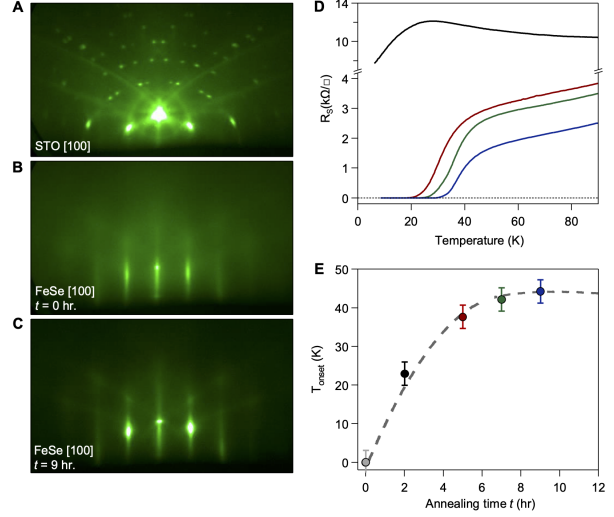


Figure 4: RHEED images along the [100] direction for (A) STO substrate prior to film deposition, (B) 1UC FeSe film immediately after growth, and (C) 1UC FeSe after 9 hours accumulated annealing at 450 °C. (D) Resistivity data as a function of accumulated annealing time. (E) T_{onset} as a function of accumulated annealing time.

described in Section 2.2.2, which allows us to search in the *policy space*.

We use a simple 1D learning problem to demonstrate this process. The GPR model makes a prediction throughout the parameter space based on the existing data. New data is taken at the point where the standard deviation for this prediction is the largest. In the next iteration, the latest data point is incorporated to make a refined prediction. This process is iterated until the maximum average standard deviation is below a pre-set threshold. For a 1D parameter space, the active learning process converges in less than ten iterations (Fig. 5). Notably, this sampling technique has been utilized in MBE growth of metallic oxides [46]. Since the learning target was the level of metallicity measured by the residual resistivity ratio (RRR) in a thick film (thickness ~ 100 nm), which was much less delicate and less path dependent than the task of optimizing superconductivity in 1 UC FeSe/STO, this study was able to apply a simple GPR model to efficiently sample a 3-dimensional parameter space and converge in ~ 30 iterations. Considering the 7D parameter space and the complex inter-dependencies of the data structure, we estimate that a pre-collected data size of $500 \sim 1000$ will be sufficient for the online RL training in Objective 2.

2.2 Objective 2: Design Structured Deep RL Models to Guide Self-Learning Robotic Epitaxy

We present a comprehensive self-learning MBE framework for the growth process of 1UC FeSe/STO (Fig. 6). Combining deep RL with active learning, we aim to develop a novel structured RL framework for systematic planning and real-time control, optimizing the growth process, and achieving improved material and device quality.

Metric for Success Demonstrate that the real-time controller induced by the self-learning MBE platform can improve the quality of existing design (for the FeSe growth) with less experimentation cost.

2.2.1 Deep RL for MBE

Deep RL for Real-Time Optimal MBE Control We aim to develop a system that can control the MBE growth process in real-time, similar to how a human operator constantly monitors the RHEED image and adjusts growth parameters accordingly. Naturally, we formulate the MBE growth process as a Markov Decision Process (MDP) problem, which can be solved via reinforcement learning (RL) algorithms. Chen is experienced in developing reinforcement learning algorithms for optimal control. In the context of MBE real-time control, an MDP process considers an agent taking actions such as adjusting the pre-growth and post-growth annealing process, deposition rate, substrate temperature, and other growth parameters in response to the current environment state (e.g., RHEED image patterns, growth stage). The agent receives a reward based on the distance to the target pattern or whether the target pattern is achieved and then transits to the next state. The reinforcement learning algorithm learns a policy to interact with the environment to optimize the cumulative reward received at the end of the MBE process.

Characterizing the States, Actions, and Transition Dynamics In the deep Q-learning framework [47], the

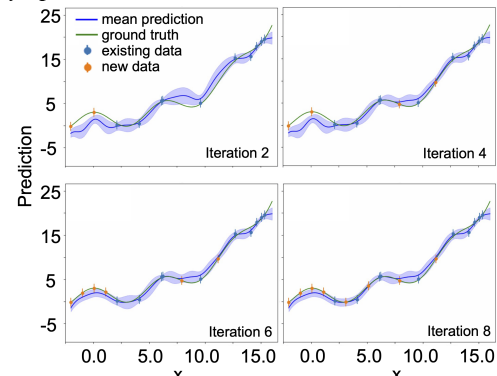


Figure 5: **Demonstration of active learning to efficiently sample the parameter space.** Here, we show the exemplary sampling process for Iterations 2, 4, 6, and 8. The Gaussian Process Regression model quickly converges to the ground truth after ~ 8 iterations.

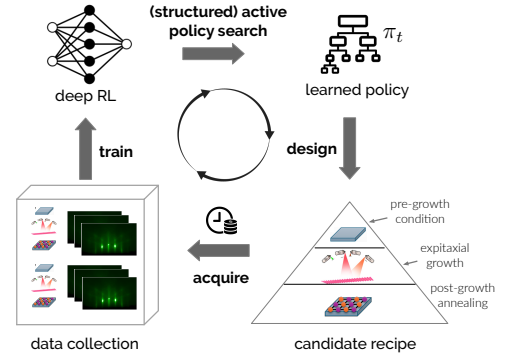


Figure 6: **Structured deep RL for adaptive recipe design in self-learning MBE** contains two core components: (1) deep RL, which constructs a collection of pre-trained MBE policies; (2) active policy search, which enables us to efficiently search over the action space with structures induced by the RL policy class.

Q function $Q(s, a)$ predicts the value of performing action a (i.e., pre-growth and post-growth annealing time, deposition rate, etc.) at state s (i.e., captured by RHEED image). In order to learn the Q function, it is crucial to have a representation model capable of effectively describing the state-action pairs (s, a) . A promising approach is to learn a representation wherein distance w.r.t. the embedding corresponds to the difference in the target Q function, computed via the Bellman equation: $Q(s, a) = r(s, a) + \max_{a'} \gamma Q(s', a')$ where γ denotes the discount factor for RL, often specified by domain experts. **In this task, we employ a Convolutional Neural Network (CNN) combined with a fully connected layer as the model architecture for learning $Q(s, a)$.** The CNN is capable of handling the spatial relationships within RHEED images and extracting meaningful features. These features can then be used to compute the RHEED image-derived metrics. To process the continuous experimental growth parameters, we can use a fully connected layer. This layer will be concatenated with the (flattened) outputs from the CNN, which enables the model to learn interactions between the features extracted from the RHEED images and the continuous experimental growth parameters. Finally, the concatenated output will be passed through a series of fully connected layers with appropriate activation functions, leading to the final output layer. This last layer will output the Q value or the reward, such as material resistance or distance to a target response pattern.

Leveraging Expert Feedback at Uncertain States Incorporating human assistance in the learning process, particularly when it comes to addressing novel and unexpected system responses, can significantly improve the overall performance and reliability of the RL algorithm. The proposed *distance to a target pattern* is not always a gold-standard reward function—when encountering abnormal or unseen states, the RL algorithm should summarize these states and ask experts (material scientists) for feedback (e.g., whether the observed pattern is better than the target pattern). By incorporating expert feedback, we can better align the RL algorithm’s decision-making process with expert knowledge, leading to a more robust and efficient control system. To effectively incorporate external feedback in the MBE growth process, **we propose to use a variant of the Proximal Policy Optimization algorithm [48], such as PPO-HF [49], to probe domain experts for additional feedback in the learning process.** PPO-HF operates by training a policy using a batch of collected data, which includes states, actions, and rewards, along with any human feedback on those actions. Such expert feedback is integrated as an additional reward signal, which guides the policy update. When the RL agent encounters an abnormal or unseen state during the MBE growth process, it can request feedback from (human) experts on the proposed action or a set of alternative actions. The expert can provide feedback on the quality of the proposed actions, and this information is used to update the policy.

2.2.2 Structured Exploration of the MBE Design Space via Active Policy Search

Despite the promise of deep RL in optimal control tasks, the training of RL agents in continuous control settings, such as enabling robotic manipulation, remains challenging due to factors such as complex environments and intricate task specifications [50, 51]. These issues lead to extensive environmental interactions, with RL agents often requiring millions of episodes to learn an efficient policy. **To improve online sample efficiency, we propose to combine (offline) RL with (online) active policy search to facilitate structured exploration of the design space (as illustrated in Fig. 6).**

Constructing Structured Candidate Design Strategies via Offline Deep RL Offline RL enables training RL policies purely from pre-collected datasets without any online exploration, translating massive offline datasets into powerful decision engines [28]. This approach is particularly impactful in real-world applications like robotics and optimal control [29, 30], where online interactions can be expensive. Motivated by these results, we will leverage the multi-stage MBE dataset collected in **Objective 1**, and use it as an offline dataset to train our candidate RL policies. We will build on a suite of off-the-shelf offline reinforcement learning algorithms, including Conservative Q-Learning (CQL) [31], Batch-Constrained Q-Learning (BCQ) [32], Offline Reinforcement Learning with Implicit Q-Learning (IQL) [33], Uncertainty-Based Offline Reinforcement Learning with Diversified Q-Ensemble (EDAC) [34], and construct a large collection of pre-trained offline policies as our candidate design strategy. Note that these design strategies are highly

structured as they are directly trained on the multi-stage MBE data underlining specific deep RL models.

Efficient Exploration of MBE design via Active Policy Search Given a collection of (pre-trained) candidate design policies, we propose to follow an optimism-based active exploration strategy to probe the MBE design space efficiently. Recently, **Chen** have investigated an active RL problem, where the active learner has access to a collection of suboptimal policies (e.g., pre-trained from offline data) [52]. We have demonstrated that one can significantly accelerate RL (i.e., via a policy optimization algorithm [49]) by jointly reasoning over which states to *explore*, as well as which pre-trained policy to *exploit* (see Fig. 7) at any given state. Built upon such preliminary results, we will investigate a novel active policy search framework to improve the sample efficiency of RL for MBE. Specifically, we will employ *deep ensembles* [53] as an effective tool for uncertainty quantification. By aggregating predictions from a diverse set of models, deep ensembles capture the inherent epistemic uncertainty. In our architecture, we train an ensemble of Q -networks, leveraging the variance of their predictions to quantify uncertainty. We can then leverage the upper confidence bound of the Q -value derived from the deep ensembles to guide optimistic exploration. Alternatively, we will also explore ensemble sampling, where we learn the value function itself through a model-based RL framework. By randomly sampling a member from the ensemble and greedily rolling out a trajectory based on the corresponding model, it amounts to a principled approach that encourages exploration in a manner akin to posterior sampling [54, 55, 56, 57]. By incorporating these uncertainty estimates or randomizing exploration into the decision-making process, we can enhance the robustness and efficiency of the MBE growth process and achieve better material quality.

2.3 Objective 3: Develop Preliminary RL Models for Real-Time Control in Robotic Mini-Epitaxy

Mini-MBE Superconducting quantum devices are traditionally manufactured in a clean room using tens to hundreds of lithographic processes. This not only introduces low efficiencies but also leads to a high density of defects and impurities, contributing to the rapid dephasing of quantum states. Mini-MBE is a potentially revolutionary technology developed by the **Yang** laboratory to integrate materials synthesis and device nanofabrication in one step. By confining molecular beams in nanoscale nozzles and coupling the substrate to a piezoscaner, we directly print devices by programming the piezoscaner's movement. The substrate temperature is controlled via a laser heater which heats up the substrate from the back side. To ensure thermal isolation between the substrate and the underlying piezoscaner, a patent-pending meta-material thermal insulator was developed by the **Yang** laboratory. This is equivalently a 3D printer for superconducting quantum circuits. We will focus on fabricating superconductor-insulator-superconductor heterojunctions, the so-called *Josephson junctions*, which are foundational to all forms of contemporary designs of superconducting qubits. In Aluminum-based Josephson junctions, the tunneling insulator barrier is made by oxidizing the surface layer of printed Al structures. With current focused ion beam technologies, it is feasible to fabricate nozzles with an opening diameter down to 100-200 nm, approaching the diffusion length of Aluminum at room tempera-

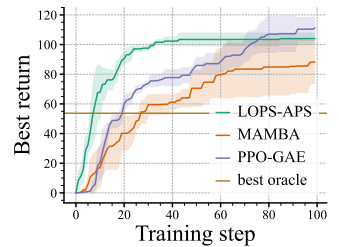


Figure 7: **Active learning improves sample efficiency of RL.** Our prior work [52] shows that activating state and action exploration (in green) allows a sample advantage over baselines.

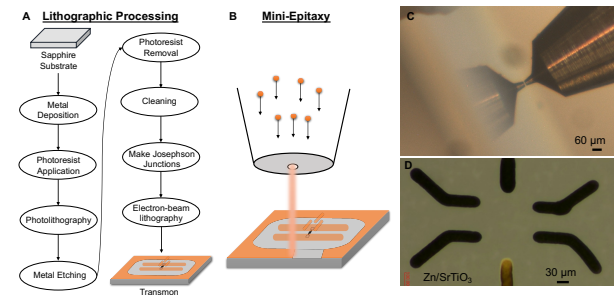


Figure 8: **Miniaturized molecular beam epitaxy (mini-MBE) for printing superconducting quantum circuits** (A) Protocol for traditional lithographic processing to fabricate a transmon. (B) Schematic for mini-MBE to print a transmon. (C) Photograph of a microscopic nozzle placed on top of a substrate. (D) Preliminary printing results of a Zn pattern on a SrTiO_3 substrate.

a patent-pending meta-material thermal insulator was developed by the **Yang** laboratory. This is equivalently a 3D printer for superconducting quantum circuits. We will focus on fabricating superconductor-insulator-superconductor heterojunctions, the so-called *Josephson junctions*, which are foundational to all forms of contemporary designs of superconducting qubits. In Aluminum-based Josephson junctions, the tunneling insulator barrier is made by oxidizing the surface layer of printed Al structures. With current focused ion beam technologies, it is feasible to fabricate nozzles with an opening diameter down to 100-200 nm, approaching the diffusion length of Aluminum at room tempera-

ture [58]. This precision is sufficient for printing state-of-the-art Aluminum-based Josephson junctions and superconducting qubits such as the transmons [59, 60], as the width of the tunneling barrier is defined only by the depth of oxidation. To print FeSe-based Josephson junctions, we will need special substrates such as the bi-crystal STO [61]. These substrates provide a nanometer- or sub-nanometer-wide gap to serve as the tunneling barrier to accommodate the short coherence length of high-temperature superconductors. Since FeSe is grown in the “absorption-control” mode, only the Fe flux needs to be confined through a nano-nozzle while the Se flux serves as the reactive agent across the entire device. **In this Objective, we will mainly focus on using customized RL to ensure the optimal printing quality of FeSe superconducting quantum devices.** It is worth noting that such a programmable mini-epitaxy setup is much beyond the traditional shadow mask technique, which was also realized by PI Yang for FeSe growth [62] but was used to print only fixed structures defined by the shadow mask. The robotic mini-epitaxy setup, on the other hand, will allow real-time programmable printing of superconducting devices without resorting to nanofabrication.

Learning Mini-MBE Control Policy In addition to the growth parameters defined in Section 2.1, we will need to control the printing speed v_p and the nozzle-substrate distance d_{ns} . Given the limited time and resources of the FMSG, we will utilize real-time optical microscopy with resolutions $\sim 1 \mu\text{m}$ (Fig. 8D). The uniformity of the printed FeSe structure will be measured by the optical reflectivity or transmissivity, serving as low-fidelity characterization data of the intermediate reward, to be fed to a structured deep RL model developed by Chen (similar to the model described in **Objective 2**). The RL model will generate instructions for the mini-MBE setup to adjust specifically v_p and d_{ns} to ensure the uniform printing of FeSe structures. The rest of the growth parameters will be determined from the optimized values in *Objectives 1 and 2* as a coarse-grained environmental condition. After we complete the entire printing process, the device will be taken out of the mini-MBE system and examined by high-resolution atomic force microscopy (AFM) or scanning electron microscopy (SEM). The AFM and SEM data will provide the *ex situ* expensive reward for the RL model. We will also measure the I-V relationship and critical current density to fully characterize the printed Josephson junction.

Joint Optimization of the Growth Conditions and

Mini-MBE Control Policy We propose to develop a **bi-level RL framework** that incorporates a fine-grained learning agent for performing mini-MBE control and a coarse-grained learning agent for optimizing the rest of the growth parameters in *Objective 1*, as illustrated in Fig. 9. The fine-grained learner will focus on learning and optimizing policies within each environmental condition, while the coarse-grained learner will aim to design a policy to select the most promising environments. Bi-level RL has been studied primarily in meta-learning and multi-task RL settings [35, 36, 37, 38, 39]. Notably, Meta-Learning Shared Hierarchies (MLSH) [35] integrates bi-level hierarchical RL with meta-learning, and the option-critic architecture [36] utilizes a two-tier system to handle extended actions. Furthermore, VariBAD [38] combines meta-learning and Bayes-adaptive reinforcement learning into a bi-level structure. Our problem naturally fits into this setting, and we will explore such established bi-level RL approaches to streamline the optimization of the full mini-MBE pipeline.

Impact on Cyber- and Eco-manufacturing of Quantum Devices If successful, this *Objective* will potentially introduce an AI-based robotic system to print superconducting quantum circuits with ultimate control. It will be a paradigm-shifting milestone to transform how superconducting qubits and quantum computers are fabricated. Moreover, due to the lithography-free printing, the robotic mini-epitaxy will largely circumvent the significant financial, energy, and climate costs associated with clean-room fabrication of superconducting

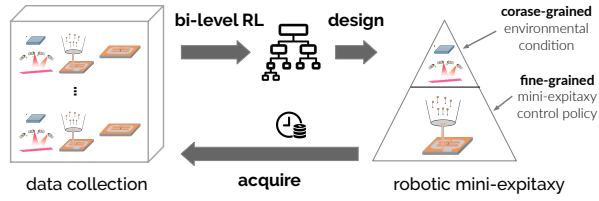


Figure 9: **Adaptive recipe design via bilevel deep RL.** At each round, the (high-level) coarse-grained RL agent determines the environmental condition and interacts with the (low-level) fine-grained mini-MBE controller to collect a new trajectory. The goal is to learn an optimal control policy for robotic mini-epitaxy jointly.

qubits, leading to a broad impact in the eco-manufacturing of quantum devices.

2.4 Preliminary Results: A Robotic Epitaxy Setup for Manufacturing Silver Beam Splitters

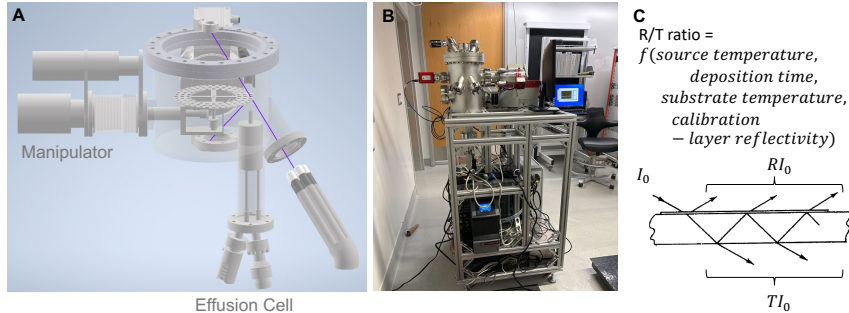


Figure 10: A robotic epitaxy prototype for synthesizing silver-film beam splitters. (A) The design concept of the prototype system consisting of a motorized manipulator which can deposit 90 beam splitters, one silver effusion cell, and an *in situ* optical reflectivity and transmissivity setup using 5 laser pointers at different wavelengths. (B) The setup in the Yang lab. (C) The concept of controlling the source temperature, deposition time, substrate temperature, and calibration-layer reflectivity (R_c) to achieve specific splitting ratios at user-defined wavelengths.

Here, we demonstrate the principles of ML-guided robotic thin-film manufacturing using a small-scale testing MBE system constructed by the Yang lab at the University of Chicago. We define the growth task as manufacturing silver thin films as optical beam splitters with user-specified splitting ratios and operational wavelength. Compared to the fabrication of FeSe, this growth task involves only one effusion cell and is less sensitive to the initial and intermediate growth stages. The growth *recipe* can be defined by source temperature, growth time, substrate temperature, and calibration-layer reflectivity. Instead of using RHEED data as the metric of the film quality, we used *in situ* reflectivities and transmissivities measured at a few discrete wavelengths.

2.4.1 Prototype Hardware: Automated Sample Transfer and Real-Time Data Output

As a preliminary proof-of-concept for more complex manufacturing tasks, we constructed a prototype system in the **Yang** laboratory (Fig. 10). Importantly, all the sample manipulation, effusion cell control, and characterization data collection have been integrated into a centralized, home-made mission-control user interface which is fully customizable. Our innovative design of a carousel-based sample manipulator puts individual substrates in a circular pattern, and utilizes the rotational and translational degrees of freedom to automatically move from one sample to the next. Real-time characterization data is taken using the laser reflection and transmission setup, generating reflectivity and transmissivity of each fabricated beam splitter at > 5 wavelengths. This setup is thus capable of completing the sample transfer, effusion cell control, deposition control, and characterization data collection completely without human intervention. Notably, for each round of deposition, we fabricate a total of 90 samples with systematically varied growth recipes, generating > 450 data points for the reflectivities and transmissivities at different wavelengths.

Even though this is a different deposition task, we emphasize that the ML framework we established in this preliminary robotic system is directly transferrable. Here we define the key parameters for a *recipe*, and the nature of the *characterization data*.

Recipe. The recipe of fabricating a silver-film beam splitter is defined by the source temperature, deposition time, substrate temperature, and calibration-layer reflectivity (R_c). The source (silver) temperature is varied between $700 \sim 900$ °C, which corresponds to the typical vapor pressure of $10^{-5} \sim 10^{-3}$ mbar. The deposition time is varied between 0 and 10 minutes, considering the typical deposition rate of 1 nm/min. With a N₂-based cryostat, the manipulator adjusts the sample temperature between 100 and 300 K. As explained in Section 1, hard materials synthesis is sensitive to the initial condition of the substrate. In our prototype, considering the relatively simple task of predicting and optimizing the reflectivity/transmissivity

ratios, we grow a calibration layer of ~ 1 nm before proceeding to each full growth cycle. The reflectivity of the calibration layer (R_c) is a parameter encoding the initial condition of the substrate, and allows us to train a rather simple GPR model to predict the optical properties of much thicker silver films (> 10 nm). We emphasize that this is only valid due to the simple task of optimizing optical constants. For more involved tasks such as optimizing the absorption spectrum for an extended range of wavelengths, a structured RL model will be required to account for the high sensitivity to the initial and intermediate conditions.

Characterization data. The goal of the beam splitter fabrication is to realize a user-defined beam splitting ratio at a desired wavelength. The beam splitting ratio is a complex function of the film thickness, flatness, morphology, and other parameters. Practically, since the splitting ratio is always a smooth function of the laser wavelength, we take real-time reflectivities and transmissivities at a few discrete wavelengths (e.g. 405 nm, 525 nm, 640 nm, 685 nm, 830 nm). We use an Active Learning algorithm to train a GPR model, which always searches for the parameter space with the highest standard deviation for predictability. A fully converged GPR model allows us to predict the growth recipe to achieve the user-defined targets.

2.4.2 Active Learning of Multi-Dimensional Data

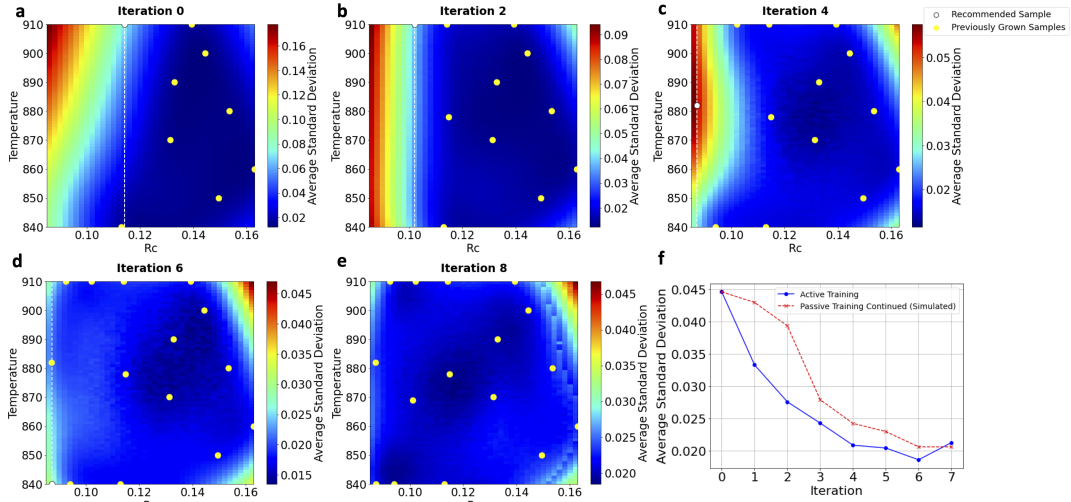


Figure 11: **Training a Gaussian Process Regression (GPR) model using active learning.** (a-e) Iteration-by-iteration evolution of the average standard deviation map as a function of the calibration layer reflectivity (R_c) and the effusion cell temperature (°C). The algorithm searches for the parameter space with the largest prediction error. (f) Comparison between the performance of active learning versus that of passive learning.

The preliminary robotic epitaxy setup operates in two stages. At the **training stage**, the robotic system generates the training data by varying the growth recipe. Here we adopt the *Active Learning* procedure developed by **co-PI Chen**, as described in Section 2.1.2. New growth conditions will be explored at the point with the largest average standard deviation, indicating the least predictability. Our results show that after 6 or 7 of such active training iterations, the average standard deviation is quenched to < 0.02 for the prediction of reflectivity/transmissivity ratios of order 1 (Fig. 11f). After the active training of the GPR model, the robotic epitaxy system starts the **deployment stage**. A user will specify the beam splitting ratio at a particular wavelength. The GPR model generates instructions for the system to manufacture the corresponding beam splitter. If the characterization of the first product yields a predicted reflectivity/transmissivity ratio that deviates from the user-specified value by more than the pre-defined threshold, the robotic system adds the new characterization data to refine the GPR model and makes refined predictions for the next beam splitter. This procedure is iterated until converged.

Structured RL is not needed for the simple task of manufacturing user-specified beam splitters. However, one can envision that the silver deposition can be separated in several stages, each of which uses a distinct deposition condition. Such a multi-staged manufacturing process can lead to numerous possibilities such as

the optimization of the optical reflectivity/transmissivity at not only one wavelength but within a continuous wavelength range. A multi-layered silver coating can lead to a user-specified frequency filter, such as a low-pass filter, and is subject to future investigations. Nevertheless, the success of using active learning to model and predict recipes for silver thin films with user-specified optical properties demonstrates the feasibility for us to apply similar methodologies to the more complex task of manufacturing superconducting quantum materials and quantum circuitry.

2.5 Teaming Plan

2.5.1 Management of the Current Team

PI Yang is a materials scientist who specializes in the growth of chalcogenide thin films. **Yang** has demonstrated success in fabricating FeSe/STO thin films using traditional human-driven MBE [20, 26, 27, 63], and will be responsible for the hardware implementation of the robotic epitaxy and robotic mini-epitaxy. The **Yang** group will utilize the existing FeSe MBE to perform systematic synthesis of FeSe/STO, feeding large volumes of data to the structured RL models. **Co-PI Chen** is a computer scientist who leads various large-scale collaborations on AI-in-Science within and beyond the UChicago campus. **Chen**'s previous work has demonstrated that ML can successfully optimize the design parameters for various scientific applications, including a plasmonic filter design [64, 65], cosmic experimental design [66], and biochemical engineering [67]. The **Chen** group will be responsible for analyzing the data from the **Yang** group, and design ML and RL models to predict the optimal growth recipe. The two groups will coordinate through monthly team meetings and frequent interactions via informal meetings. **Yang** will keep track of the overall project timeline and ensure that the team anticipates and addresses bottlenecks proactively.

2.5.2 Team Expansion and Industry Collaboration

In anticipation of expanding the project into a Future Manufacturing full proposal, the team will actively seek opportunities to partner with materials scientists, physicists, engineers, and computer scientists at the University of Chicago. We have already started this effort through the conversation with Prof. Supratik Guha at the Pritzker School of Molecular Engineering and Dr. Jie Xu at Argonne National Laboratory (letters of collaboration appended). We will further crystallize the intellectual conversations on AI-driven material and device fabrication by organizing an annual workshop inviting interested faculty members, national lab scientists, industrial leaders, as well as postdoctoral scholars and graduate students to a half-day intellectual exchange forum. It is one of our most important Broader Impacts objectives to seed and grow this intellectual conversation, which will eventually lead to a group of 5~6 principal investigators to form the basis for a Robotic Quantum Manufacturing hub in the Midwest region.

2.6 Risk Assessment and Mitigation

Leveraging **PI Yang**'s substantial experience in the FeSe/STO fabrication [20, 26, 27, 63], the risk for collecting systematic RHEED data from 1 UC FeSe/STO films is low. Moreover, the structured RL model should be able to mitigate the risk due to substrate-to-substrate differences. Nonetheless, it is known that STO substrates from different vendors can exhibit systematic differences beyond the standard substrate-to-substrate variation. To mitigate this risk, we will coordinate with the substrate vendor (Shinkosha, Co. Ltd.) to obtain a large number of consistent substrates from the same batch. For *Objective 3*, the manufacturing modality of mini-MBE is fundamentally new and carries a higher risk. For instance, clogging of the nanoscale nozzle can be a significant risk. To mitigate this risk, we have designed a mechanism to change nozzles *in situ* without breaking vacuum. In addition, it is unclear whether sufficiently high-resolution optical images can be taken in real time while the nanonozzle moves across the substrate. To mitigate this risk, we will build a special vacuum chamber with an “inverse” vacuum tube, allowing the objective lens of the microscope to be < 30 mm to the printed device and leading to high-quality images similar to those generated by a regular microscope.

2.7 Project Timeline

Tasks	Year 0	Year 1	Year 2
Objective #1: Build the Multi-Stage Epitaxy Database for Structured RL			
Objective #2: Design Structured Deep RL Models to Guide Self-Learning Robotic Epitaxy			
Objective #3: Develop Preliminary RL Models for Real-Time Control in Robotic Mini-Epitaxy			
Broader Impact Objectives: annual workshop, course development, outreach.			

3 Results of Prior NSF Support

PI: Shuolong Yang is supported by *NSF DMR-2145373*; Amount \$687,153; 02/2022-01/2027; “**CAREER: Tuning Topology and Strong Correlations for the Next Generation of Topological Superconductors**”.

Intellectual Merit: This project will provide a complete synthesis and physics understanding of the novel topological superconducting thin films $\text{FeTe}_x\text{Se}_{1-x}$ on oxide substrates. We will provide answers to a number of pressing issues in topological physics, such as (1) the nature of the topological phase transition, (2) the mechanism of correlation-enhanced superconducting order, and (3) how to realize nonabelian anyon statistics. Broader Impacts: The knowledge and expertise developed in this project will not only be ground-breaking in the development of topological quantum computing, but will also lead to educational and outreach activities under the theme of “*Immersive Quantum Material Education*.” **Publication:** [68, 69]

Co-PI Chen is currently supported by three NSF grants, and the most related is *NSF-2037026*; Support period: 01/01/2021-12/31/2025; Total amount: \$10,000,000 (in total); Chen’s share: \$375,000; “**FMRG: Manufacturing ADvanced Electronics through Printing Using Bio-based and Locally Identified Chemicals**”. Intellectual merit: Develop novel machine learning algorithms for optimizing the design of the manufacturing supply chain from precision agriculture/hydroponics to advanced biodegradable and recyclable electronics. Broader impacts: An open-sourced democratized manufacturing prototype that enables distributed manufacturing of low-cost printable electronic devices using locally identifiable resources such as bio-based materials derived from plants. Educate and train a wide audience on the proposed future manufacturing using evidence-based practices grounded in experiential learning. **Publication:** [70, 71].

4 Broader Impacts

This project will potentially transform how to manufacture superconducting materials and devices in the future, and build a direct interface with manufacturing in industry. In particular, the technology of robotic mini-epitaxy will lead to direct applications in optical devices, superconducting devices, and quantum information devices. We will work closely with the Polsky Center for Entrepreneurship and Innovation at the University of Chicago to properly disclose the technology through appropriate channels. We are aware of the disconnect between academic and industrial sectors on the MBE activities, and will host an annual *Robotic Quantum Ensemble* workshop to invite academic and industrial leaders as a forum for not only our team members, but also the extended collaborative network and industrial partners to exchange ideas. We will also leverage the geographical locations of South Side Chicago, which is integrated with the African American community, and provide outreach opportunities to engage the under-represented minority students. This project will enable us to educate, train, and connect the next-generation workforce for quantum materials scientists, which is key to reviving the American manufacturing industry in the Midwest region.

4.1 Education and Workforce Development

Graduate and Undergraduate Student Mentoring The PI and Co-PI will train the new generation of workforce by closely co-mentoring graduate and undergraduate students. It is worth noting that PI **Yang** has been mentoring a team of 3 undergraduate students to build the first robotic epitaxy prototype as mentioned in Section 2.4. One of the students is a female student. **Yang**’s group is also the only quantum materials group at the University of Chicago who has successfully recruited an African American PhD student. The students

working on this project will participate in the annual *Robotic Quantum Ensemble* workshop to directly interact with industrial leaders, which will facilitate potential matching between the students and future job opportunities in the Midwest region.

Course Development The PIs see great importance in developing courses tightly integrated with research. At UChicago, **Co-PI Chen** has already developed a new graduate course on *Bayesian Optimization and Adaptive Experimental Design*, which covers several aspects related to this proposal. We will integrate the methods investigated in this project into this course. **PI Yang** will also develop a new course “Science of Materials” which aims at starting with the core solid-state principles and going beyond the standard single-particle description at the end of the course. This course will be part of the new materials science curriculum under development within the Pritzker School of Molecular Engineering, and prepare students for more advanced quantum engineering and quantum materials studies. **PI Yang** will dedicate 30% of the new course content to frontier research topics such as advanced manufacturing, including the new paradigm of *robotic epitaxy*.

4.2 Annual Workshop: Robotic Quantum Ensemble

We will host an annual *Robotic Quantum Ensemble* workshop to invite the FMSG team members, extended collaborators, and industrial partners to join in a half-day workshop, which aims to provide a forum for the team to have close interactions and outline immediate and long-term goals for future quantum manufacturing activities. Moreover, the workshop will help broaden the impact of our FMSG project to regional materials science communities. The workshop will feature speakers from outside the team and will provide annual summaries of updates in the broad field of *smart manufacturing*. In particular, we will join force with the existing effort of AI-driven robotic synthesis of polymer materials at Argonne National Laboratory, and crystallize ideas and concepts for a regional *Robotic Quantum Manufacturing* center for both hard and soft materials. The University of Chicago has a strong interface with the manufacturing industry in the Midwest region (e.g. Veeco, 3M, Seagate). This workshop will be integrated with the broader eco-system established by The Bloch Tech Hub, which is a regional coalition of industry, academic, government, and nonprofit stakeholders with the mission to generate \$60 billion economic growth, create 30,000 quantum jobs, train 50,000 workers, and support 200 quantum companies by 2035.

4.3 Outreach Activity

UChicago Quantum Quickstart The UChicago Quantum Quickstart program is a 1-week accelerated quantum introductory workshop for students from the 9th to 11th grade. **Yang** is one of the two inaugural instructors for the 2021 program, which received 276 total applications with 11% identified as African-Americans, 22% as Hispanics/Latinos, and 1% as Native Americans. A total of ~70 students were recruited. Under this proposal, PI Yang will leverage the existing UChicago Quantum Quickstart program and incorporate frontier research results from *robotic epitaxy*. This has a particularly strong impact due to the strong presence of manufacturing in America’s Midwest region, and will encourage under-represented students to envision and pursue careers related to manufacturing from an early stage. We will use the demographics and course feedback from every summer to assess the success of this outreach event.

Physics with a Bang The Yang group has been active participants of the “Physics with a Bang” outreach program hosted by the University of Chicago community involving more than 500 participants from K-12 students and local residents. Under this project, we will utilize the compact testing robotic epitaxy system, and make a demo booth at the Physics with a Bang event. Importantly, the testing system is a fully mobile system with an uninterrupted power supply providing 6 hours of stand-alone operation. We will be able to engage with the public and let them specify the parameters for optical beam splitters and start the automatic synthesis. This will be an opportunity to showcase the amazing future promises of robotic epitaxy by directly engaging the general public. We will use the number of visitors and their feedback to assess the success of this outreach event.